Macromolecules
ARTICLE

Macromolecules **2009**, *42*, 4667–4673 **4667**
DOI: 10.1021/ma8021234

Understanding of the Plasticizing Effects of Glycerol and PEG 400 on Chitosan Films Using Solid-State NMR Spectroscopy

Attila Domján,*,† János Bajdik,‡ and Klára Pintye-Hódi‡

†*Institute of Structural Chemistry, Chemical Research Center, Hungarian Academy of Sciences, H-1025 Budapest, Pusztaszeri út 59-67, Hungary, and* ‡*Department of Pharmaceutical Technology, University of Szeged, H-6720 Szeged, Eotvos u. 6, Hungary*

Received September 19, 2008; Revised Manuscript Received May 15, 2009

ABSTRACT: Differences were found in the plasticizing effects of two commonly used softening materials on amorphous chitosan films. The plasticizing efficiencies for glycerol and PEG 400 were found to be similar in mechanical tests, but the changes in the three-dimensional H-bonded structure monitored by solid-state NMR spectroscopy were different. The analysis of Lee−Goldburg cross-polarization build-up curves demonstrated that, while glycerol decreases the mobility of the acetamide groups, PEG 400 increases it. Further, while glycerol molecules are immobilized in chitosan films, PEG 400 remains mobile in them. The results of two-dimensional (2D) $^{1}H-^{13}C$ frequency-switched Lee−Goldburg (FSLG) HETCOR experiments supported the mobility difference of the chitosan chains and suggested a specific interaction between the glycerol and the glucosamine units. Our findings were supported by density functional theory calculations. Overall, PEG 400 acts as an external plasticizer, while glycerol acts as an internal plasticizer.

Introduction

Chitin, poly(β-(1−4)-D-*N*-acetylglucosamine), is an extremly important and widely used polysaccharide-type natural polymer. Although this material was identified more than a century ago, chemists began to devote attention to it only in the late 1970s. Chitin is produced by a number of animals and fungi, and it is the second most abundant biopolymer after cellulose. The main sources of chitin are crab and shrimp shells, and it is readily commercially available as a byproduct of the seafood industry. Natural chitin can be modified by various biological and chemical methods. Its most important derivative is chitosan, a partly deacetylated chitin. Chitin and its derivatives have a wide range of applications in the fields of agriculture, water and waste treatment, food, cosmetics, medicine, biopharmacology, etc. More details may be found the listed reviews and the references therein.[1,2]

Chitin and chitosan are crystalline or semicrystalline materials with different allomorphs. The crystal structure is stabilized by intramolecular and intermolecular H-bonds, with the acetamide groups playing the major role in the formation of second-order bonds between adjacent chains.[3] The structures of chitin and chitosan have long been investigated by various methods;[1,2] more specific studies have been carried out in the past decade with modern instrumental methods such as X-ray crystallography,[3−6] infrared spectroscopy,[7] and solid-state NMR spectroscopy.[4−9]

Chitosan is widely used in pharmaceutical technology as a conventional film-coating material[10,11] and has been proposed as a component of new drug delivery systems (e.g., microparticles,[12,13] nanoparticles,[14] temperature-sensitive hydrogels,[15] gastric retentive systems,[16] wound dressings,[17] and drug-loaded mucoadhesive films[18]). Besides the nontoxic nature and biocompatibility of chitosan, its film-forming ability is an important aspect for medical applications. Films made from pure chitosan are rigid and brittle, and it is therefore important to use plasticizers in order to obtain more favorable mechanical properties. Because of the potential medical applications, the plasticizer materials must be biocompatible. The effects of different plasticizer molecules and the stability of the plasticized films have been investigated,[19−22] and it has emerged that poly(ethylene glycol) (PEG) and glycerol are the best candidates as plasticizers of chitosan films. Other small molecular organic materials have been found to be effective plasticizers, but their efficiency decreases within several weeks.[22] These two additives form relatively soft and stable (at least for several months) films with chitosan.[22] In general, these materials prevent the formation of second-order bonds between the adjacent polymeric chains, which hinders the recrystallization. The softening efficiencies of these two plasticizers are similar, but the mechanisms of plasticization seems to be different, as indicated by positron annihilation spectroscopy[23] and solid-state NMR investigations.[21,23]

Plasticizers[24] modify the mechanical properties of materials without altering their fundamental chemical character. The crystalline structures of polymeric materials are stabilized by second-order bonds, which are destroyed by plasticizers. During external plasticization only weak second-order bonds develop between the plasticizer and the polymer, while internal plasticizers are covalently bound to plasticized material. The external plasticizers can migrate in the polymer, which can lead to recrystallization of the material and a loss of elasticity.

Solid-state NMR spectroscopy is an effective technique that is widely used to characterize macromolecular systems,[25] especially amorphous and mixed systems that can not be characterized by scattering methods. One-dimensional solid-state ^{13}C cross-polarization magic angle spinning (CP MAS) measurements on chitosans have previously shown that changes in the H-bonded structure cause changes in the spectra. Even a temperature increase[8] or application of a plasticizer[21,23] leads to a partial destruction of the H-bonded network, which results in line narrowing and changes in intensity of the resonances. The two-dimensional frequency-switched Lee−Goldburg (FSLG) HETCOR $^{1}H-^{13}C$ technique provides more information as compared with the one-dimensional method by increasing the

*Corresponding author. E-mail: domjan@chemres.hu.

Published on Web 06/09/2009

resolution and additionally providing special proximities on the atomic scale. In the past 5 years, this method has been successfully used to map intermolecular interactions in various macromolecular systems.[26−32]

In the present study, Lee−Goldburg CP MAS build-up curves and 2D FSLG HETCOR $^{1}H-^{13}C$ spectra were recorded with different contact times (100 and 500 μs) in order to investigate the changes in the chain dynamics and H-bonded structure when a plasticizer is added to chitosan films.

Experimental Section

High molecular weight chitosan (CS) (1568, MW: 1840 kDa) was purchased from Giusto Faravelli (Milano, Italy). Ascorbic acid (AA), glycerol, and PEG 400 were supplied by Sigma Chemicals Co. (Milano, Italy). A fixed amount of AA was dissolved in distilled water (to obtain a molar ratio of 1:1 for AA:CS deacetylated amine groups). After its dissolution, the plasticizer was added at 1% (w/w), followed by CS to obtain a concentration of 2.5% (w/w). The deacetylation ratio was found by solution-state ^{13}C NMR (spectra not shown) to be 50%. The ratio of acetylated and deacetylated anomeric carbon signal intensities was given as 1:1. The pH of the CS + AA solution containing PEG 400 was ~4.6, and that of the solution containing glycerol was ~4.8. 3 g of each liquid was poured onto an even Teflon surface with a diameter of 3.3 cm and dried under ambient conditions (25 ± 2 °C and 50 ± 5% RH) for 24 h. The moisture contents of the dried films were 3.0 ± 0.3% for the film containing glycerol and 4.6 ± 0.3% for the sample containing PEG 400. The plasticizer content was 30% (w/w), and the ascorbic acid content was 6% (w/w) in both cases.

The force required to break unplasticized and plasticized chitosan films was determined with a strength tester and software developed in Department of Pharmaceutical Technology.[33] This device consists of a special specimen holder (20 mm in diameter) and a hemispherical stamp with a surface of 201 mm^2 and is connected to a computer via an interface; thus, not only can the ultimate deformation force be measured, but the process (force−time and force−displacement curves) can be followed. The round specimen is located horizontally and the stamp moves vertically.

Solid-state magic angle spinning (MAS) spectra of the samples were recorded on a Varian NMR System operating at a ^{1}H frequency of 600 MHz with a Chemagnetics 3.2 mm narrow-bore triple-resonance T3 probe in double-resonance mode. The spinning rate of the rotor was in all cases 10 kHz. Lee−Goldburg cross-polarization ^{13}C spectra[34,35] were collected with different contact times (100−3000 μs) so as to suppress homonuclear ($^{1}H-^{1}H$) dipolar interactions. The ^{13}C spectra were deconvoluted with the DMFIT software.[36] 2D FSLG HETCOR $^{1}H-^{13}C$ spectra[34] were recorded with different contact times (100 and 500 μs). The FSLG scaling factor was 0.53. SPINAL-64 proton decoupling[37] with a strength of 83 kHz was used during the acquisition in all cases. The measurement temperature was 25 °C, and adamantane was used as external chemical shift reference (38.55 and 29.50 ppm). The ^{1}H and ^{13}C pulse lengths were 3 μs, and a recycle delay of 5 s was used for all experiments. The FSLG HETCOR spectra were recorded with 24 transients and 256 increments in the t1 dimension.

Results and Discussion

The aim of this work was to study the effects of two commonly used plasticizers on the H-bonded structure of chitosan films and to demonstrate the efficiency of the frequency-switched Lee−Goldburg HETCOR ($^{1}H-^{13}C$) technique on highly amorphous biopolymers. As shown previously, both glycerol and PEG 400 are promising candidates for the softening of chitosan films.[20,22] Plasticizing efficiency most probably depends on numerous parameters, such as the origin of the chitin, the deacetylation ratio, the concentrations of additives, and the moisture content. In view of these factors, it is difficult to compare different results from the literature.[20,22] In our investigation, the breaking force was measured with three independent film samples. Both glycerol and PEG 400 were found to be good plasticizers; PEG 400 proved to be a better softener of chitosan films. The breaking forces were established to be 39.4 ± 4.1 N for glycerol-containing films and 48.5 ± 3.2 N for PEG 400-containing samples. Films of pure chitosan are very rigid and brittle, making it impossible to measure the breaking force with the applied instrumentation.

In general, the Lee−Goldburg (LG) homonuclear decoupling technique suppresses the X−H−H three-spin cross-polarization, and the cross-polarization can occur only through an X−H dipolar mechanism. This enhances the resolution in the ^{1}H dimension for correlation techniques, and the resolution of cross-polarization magic angle spectra can be improved due to elimination of the proton−proton dipolar interactions. The utility of the $^{1}H-^{1}H$ decoupling method has been demonstrated for crystalline materials, where the proton−carbon distances can be determined from the LG CP build-up curves with good accuracy.[38] Briefly, magnetization from the ^{1}H directly bonded to ^{13}C is transferred to the ^{13}C in a very short time (~100 μs), while transfer of the magnetization from nearby, but not directly bonded, protons takes a definitively longer time. $^{1}H-^{13}C$ proximities can be established by using heteronuclear correlation sequences with different contact times.

Lee−Goldburg cross-polarization spectra were recorded and deconvoluted with the DMFIT[36] software. The assignment of ^{13}C signals was based on literature data.[6,9] Even when homonuclear decoupling is used during the CP process, the resonances observed are relatively broad because of the amorphous structure of the chitosan film. Nevertheless, the signals are narrower when no homonuclear decoupling was used during the CP. During the acquisition SPINAL-64 heteronuclear decoupling were used with the same power in both cases. The line narrowing was found to be 4−6% for the methyl and carbonyl signals. For the deconvolution process the chemical shift values were fixed, and the line width and the amplitude were fitted. Gaussian-shaped lines were used for both chitosan and plasticizer signals. Deconvolution could be achieved with good accuracy, as shown in Figure 1. The error in the fitted parameters was typically < 2%. The resonances of the plasticizers can be clearly detected beneath the signals of the chitosan.

Cross-polarization build-up curves are constructed by varying the contact time and plotting peak intensity vs contact time. From the shapes of these curves, information on the proton environment of the carbon atoms and their mobility can be obtained. Directly bonded $^{1}H-^{13}C$ pairs generally result in oscillatory LG CP build-up curves, which can explain the shapes of the measured build-up curves.[38] In our case, oscillatory behavior was only partly observed because of the complexity of the H-bonded network in the sample. The frequency of the oscillation depends on the C−H distance; therefore, the contribution of the different environmental protons to the cross-polarization cannot be estimated in these amorphous materials. There are numerous possibilities to form intra- and intermolecular H-bonds between chitosans OH, NH, and carbonyl groups and the plasticizer molecules. These secondary bonds are strong and stable, but they are weakened by the presence of plasticizer molecules, as revealed by the mechanical characterization of the films. As Figure 2 shows, the intensity of the cross-polarization signals falls rapidly at short contact times, except for those of the carbonyl and the methyl resonances. The CP kinetics of the methyl and carbonyl groups are different from those of all other carbons because the methyl groups rotate very fast at room temperature and the carbonyl atom has no directly bonded protons.

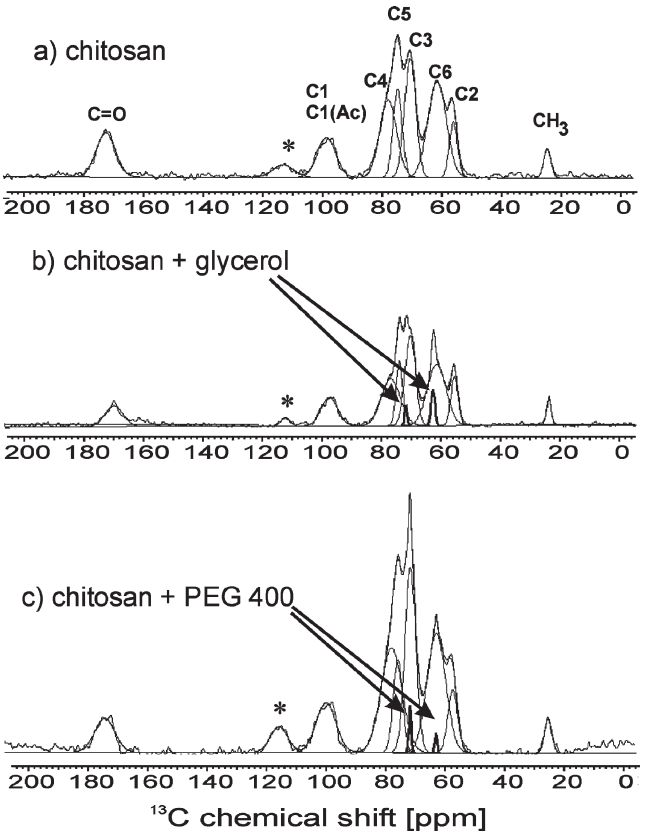

Figure 1. Lee–Goldburg cross-polarization ^{13}C spectra of pure and plasticizer-containing chitosan with a contact time of 500 μs. The signals relating to the plasticizers are indicated with arrows. The asterisks denote the spinning sideband of the carbonyl resonance.

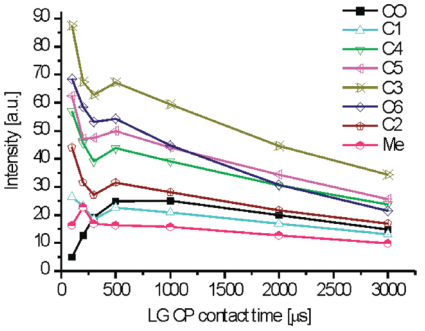

Figure 2. LG CP build-up curves of the chitosan signals. The intensity values are the results of deconvolution of the LG CP spectra.

The build-up curves are similar for the plasticizer-containing film samples, except that the carbonyl and the plasticizer signals behave differently. From the changes in these build-up curves, it is possible to determine whether the chitosan polymer chains exhibit greater or lesser mobility when plasticizers are present in the chitosan films. The plasticizer materials are expected to modify the rigid structure of the chitosan films by destroying the intermolecular H-bonds between the polysaccharide chains, and at the same time they can form new H-bonds with chitosan. This in turn leads to higher mobility of the chains. The change of the mobility of the molecules influences the cross-polarization behavior of the carbon atoms.

The more mobile a carbon is, the more slowly it relaxes. Changes in mobility of chitosan polymer chains can be monitored most clearly by analysis of the LG CP build-up curves of the carbonyl atoms (Figure 3). The acetamide group plays an important role in the formation of intermolecular bonds between

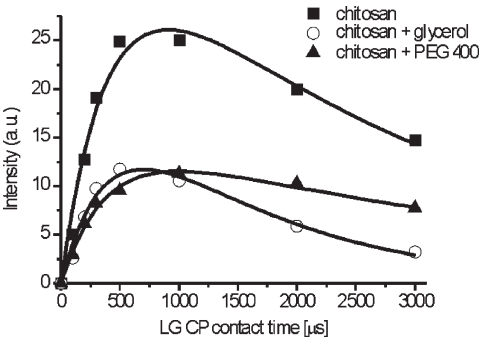

Figure 3. LG CP build-up curves of the carbonyl resonances. The curves are the fitting results of eq 1.

Table 1. Fitting Results of the Carbonyl LG CP Build-up Curves with Eq 1

sample	T_{CH} (ms)	$T_{1\rho}$ (ms)	M_0	R^2
chitosan	0.5 ± 0.1	2.8 ± 0.8	42 ± 10	0.98
chitosan + glycerol	0.6 ± 0.3	1.3 ± 0.4	29 ± 14	0.97
chitosan + PEG 400	0.4 ± 0.1	4.1 ± 0.5	16 ± 2	0.99

adjacent chains, and the oscillatory behavior of the LG CP build-up curve of the carbonyl atom is less dominant.[38] The curves were fitted with a simplified expression which enables determination of the changes in the environment and relaxation time of the H atoms:

$$M(t) = \lambda^{-1} M_0[1 - \exp(-\lambda t/T_{CH})] \exp(-t/T_{1\rho}) \quad (1)$$

where $\lambda = 1 + (T_{CH}/T_{1\rho}) - (T_{CH}/T_{1\rho})$, $M(t)$ is the magnetization at contact time t, M_0 is the initial magnetization, T_{CH} is the time coefficient of the cross-polarization (the time it takes for magnetization to be transferred from ^1H to ^{13}C), and $T_{1\rho}$ is the relaxation time in the rotating frame.

This equation describes the experimental build-up curves with good accuracy; the R^2 values of the fit were found to be close to 1. The errors in the fitted parameters are relatively large, but the differences between the investigated samples are sufficiently large to allow conclusions regarding the cross-polarization kinetics. This equation is valid only in a regime of fast molecular motion, but it qualitatively describes the experimental LG CP build-up curves and permits comparison of the fitted parameters. The cross-polarization time coefficients (T_{CH}) are the same within experimental error, meaning that the proton environment of the carbonyl atoms does not change significantly when plasticizer is added to chitosan films. It also means that the carbonyl atom accept polarization predominantly from the chitosan H atoms. The contribution of different protons to the carbonyl ^{13}C polarization cannot be estimated because of the complexity of the system; thus, the fitted T_{CH} values furnish only a little information about the proton environment. The $T_{1\rho}$ relaxation time decreases when glycerol is added to the chitosan film and increases when PEG 400 plasticizer is added to the system. This indicates that glycerol decreases the mobility of the carbonyl atom environment, whereas PEG 400 increases the mobility. This surprising observation can be explained by the changes in the amorphous structure of the chitosan films. The structures of pure chitin and fully deacetylated chitosan are stabilized by numerous intermolecular H-bonds. They are therefore crystalline materials and their solid-state NMR spectra consist of sharp resonances.[6,19] Solution-cast, partly deacetylated chitosan films have amorphous structures, and a significant proportion of the carbonyl groups do not participate in H-bonding. Glycerol is a very good H-bond donor and acceptor, and therefore it increases the number of H-bonds by donating protons to carbonyl groups and accepting chitosan OH and NH protons. On the other hand,

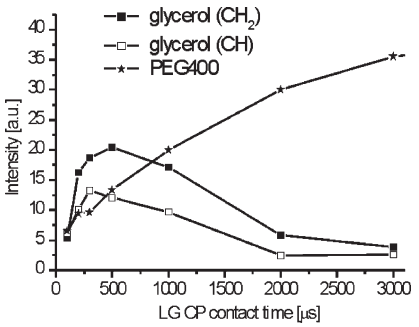

Figure 4. LG CP build-up curves of the plasticizer molecules. The curves serve as a guide to the eyes.

PEG 400 can act only as an H-bond acceptor and competes with the carbonyl groups, thereby decreasing the density of H-bonds in the chitosan film. As shown in Figure 4, the build-up curves of the plasticizer molecules support this conclusion, and the difference between the effects of the two plasticizers is clearer. The signal intensity of PEG 400 increases monotonously in the investigated contact time range, indicating the high mobility of the plasticizer molecules. The glycerol resonances behave in a different way: as glycerol is strongly H-bonded to chitosan, its cross-polarization behavior is similar to that of the carbonyl groups of chitosan.

To identify the location of H-bonds in pure and plasticizer-containing chitosan films and to monitor changes in the H-bonded network, 2D FSLG HETCOR measurements were carried out. This type of solid-state NMR experiment furnishes information on coupled $^{1}H-^{13}C$ pairs. The FSLG HETCOR technique has been successfully applied not only to small crystalline molecules but also to macromolecular systems.[9,26−32,39] Through variation of the cross-polarization contact time, $^{1}H-^{13}C$ proximities can be investigated on various length scales. With short contact times (typically < 100 μs) only the directly bonded $^{1}H-^{13}C$ pairs give cross-peaks. Short contact time FSLG HETCOR experiments are usually utilized to make precise assignments of the structure of molecule in the solid state, which is very important for the identification of different conformations and crystal forms. To investigate second-order structures stabilized by inter- and intramolecular second-order bonds, a longer contact time is needed. Cross-peaks originating from proximities on a larger length scale appear only after a contact time of several hundred microseconds. The intensity of the cross-peaks decreases as the contact time increases because of the nature of the cross-polarization process. This intensity loss is mostly determined by the $T_{1\rho}$ relaxation time of the coupled protons.

To investigate the proton carbon proximities in pure and plasticized chitosan films, 2D FSLG HETCOR spectra of the amorphous film samples were recorded with contact times of 100 and 500 μs. The spectra of the pure and the plasticizer-containing films for the short (100 μs) contact time are shown in Figure 5. With this contact time, the protons directly bonded to a ^{13}C atom and those in very close proximity to a ^{13}C atom can be investigated. Because of the amorphous structure of the films, the resolution is definitely poorer than for crystalline chitin,[9] but nevertheless crucial conclusions can be drawn. While no resonance can be assigned in the one-pulse ^{1}H spectra,[23] the resolution is improved in the ^{1}H dimension of the HETCOR spectra. Methyl (~2 ppm) and C1 (~3.5−4 ppm) trivial cross-peaks can be clearly assigned. The amide NH proton (~6.8 ppm) cross-peak with C6 carbon appears for the plasticizer-containing samples, too, and is the only observable coupling which originates from not directly bonded $^{13}C-^{1}H$ proximity. Since the interchain connectivities are hindered in plasticized polymeric materials, this proximity is due to neighboring monomer units in a chain. The signals of C2−C6 carbons are very broad because of the numerous couplings in the glucose ring, but they display some narrowing in the plasticizer-containing samples. This narrowing is brought about by the increasing mobility of the chains. The increased mobility of the chains caused by the plasticizer materials can be monitored more unambiguously by using the cross-peaks of the methyl and the anomeric C1 carbons. In the plasticized samples, the intensity of these decreases and they become narrower. This effect is larger for the PEG 400 film than for the glycerol-containing film, which is in good agreement with the results of mechanical measurements. Signal narrowing in the PEG 400-containing film allows two overlapping C1 peaks to be resolved, which can be assigned to the C1 resonances of glucosamine (99.7 ppm) and *N*-acetylglucosamine (95.5 ppm). The intensity of the methyl cross-peak decreases similarly to that of the C1 signal, and the methyl carbon signal becomes narrower. While the signal narrowing indicates higher mobility, the intensity decrease suggests a decrease in the heteronuclear couplings: the contribution of not directly coupled protons to ^{13}C polarization decreases in consequence of the decomposition of the H-bonded network structure.

Increase of the contact time to 500 μs results in suppression of the cross-peak intensities originating from the direct $^{13}C-^{1}H$ couplings and increases the intensities of the couplings from protons in close proximity to, but not directly bonded to, carbon atoms. New cross-peaks appear in the spectra of pure and glycerol-containing films, which suggests local order in the range of several angstroms, as shown in Figure 6. In the spectra of the PEG 400-containing film, fewer cross-peaks are present, which indicates a less ordered structure. In the glycerol-containing sample, the intensity of the anomeric C1 carbon cross-peaks decreases, and two resonances due to glucosamine and *N*-acetylglucosamine C 1s can be resolved (similarly as for the PEG 400-containing film measured with a shorter contact time). Couplings of the carbonyl ^{13}C with H2 proton can be seen only for the untreated and the glycerol-containing chitosan films. This cross-peak is not present for the PEG 400-containing sample because, as a result of the lower H-bond density, this C has higher mobility and is not constrained to stay near H2. This agrees very well with the CP kinetics of the carbonyl signal (Table 1). Comparison of the methyl signals for the three different samples also indicates differences in the mobilities of the acetyl groups in these films. The presence of a cross-peak between the methyl carbon atom with the directly bonded (2 ppm) and a chitosan proton (~3.5 ppm) indicates lower mobility (i.e., a higher H-bond density), while its lack indicates higher mobility and a lower H-bond density. Because of their ability both to donate and to accept H atoms so as to form H-bonds, the acetamide groups of chitosan play an important role in forming the three-dimensional network structure of chitosan films. As shown by the schematic picture given by Kameda et al.,[8] the amide NH proton is in close proximity to C3 carbon if the carbonyl group forms an H-bond with the OH group on C6 carbon. The cross-peak between C3 and the amide NH proton appears for all three samples, indicating the presence of second-order bonds. However, the intensity of this signal is smaller for the PEG 400-containing film and more intense for the glycerol-containing film.

New cross-peaks appear in the HETCOR spectra of the glycerol-containing film (Figure 6b) indicating higher order on the local scale relative to the other two film samples. The two smaller peaks, close to the C3-NH cross-peak, can be assigned to coupling of the glycerol carbons with the amide NH proton. These peaks clearly show that glycerol is in close proximity to the chitosan polymer chains. This connection is most probably stabilized via H-bonds between the glycerol and polymer molecules. A similar connection was not found for PEG 400. Additionally, a new signal emerges in the proton dimension, at

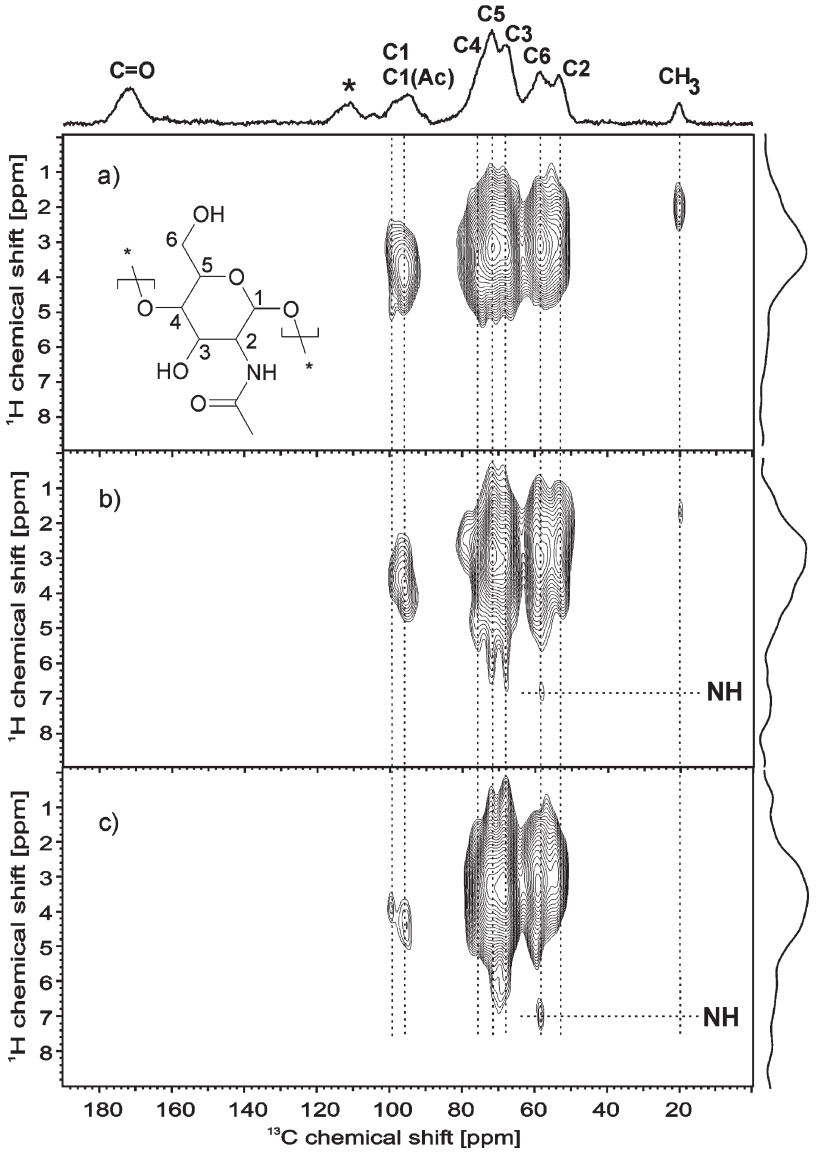

Figure 5. FSLG HETCOR spectra with a contact time of 100 μs (a, chitosan; b, chitosan + glycerol; c, chitosan + PEG 400). The contour levels are the same for all three spectra.

5.6 ppm, which can be seen only in this spectrum. This signal gives a cross-peak with C1 and the carbonyl atom; other connections with C2−C6 carbons cannot be identified because of the poor resolution. This signal most probably relates to one or more OH groups because it does not appear in the spectra recorded with a contact time of 100 μs, and its chemical shift is larger than all the CH shifts for the polymer or glycerol.

The differences between the amide NH proton proximities in the two types of plasticizer-containing films allow conclusions concerning the mechanism of the plasticizing effect of the two plasticizer materials. Glycerol molecules are probably bound to the acetamide group of chitosan by H-bonds, which prevent the acetamide groups from forming interchain H-bonds with other chitosan molecules, and leads to breakdown of the intermolecular connectivity between the polysaccharide chains. No stable connection was found between the PEG 400 molecules and the polysaccharide chains, but the H-bonds formed by the amide groups are decreasing. We therefore hypothesize that PEG 400 acts much more as an external plasticizer, while glycerol acts as an internal plasticizer for chitosan films.

To investigate this hypothesis, the films were soaked in deuterated water for 1 day, and the supernatant was then analyzed by liquid-state ^{1}H NMR spectroscopy. The chitosan films did not dissolve during the investigated period (spectra not shown). In the solute (besides the ascorbic acid), both plasticizers were detected in the same amount within experimental error. We expected less glycerol than PEG 400 to diffuse out of the plasticized films, since glycerol appears to be strongly H-bonded to chitosan, while PEG 400 is not. By analysis of the solution state spectra we suggest that a large amount (almost all) of both additives was diffused out from the film samples during 1 day. This simple experiment did not differentiate between the modes of action of the two plasticizers. However, the results do suggest that, during potential medical applications, the plasticizer molecules may diffuse out from the films, which could lead to changes in the transport properties of the films (pores are formed in the insoluble films).

To investigate the interaction between glycerol and chitosan, density functional theory calculations were carried out on a simplified model system with the Gaussian 03[40] software package on the b3lyp/6-31 + + g(d,p) basis. The polysaccharide chain was modeled by one glucosamine unit, and the neighboring units were replaced with methyl groups. Although the model system is very small, it represents the important part of the chain from the aspect of the H-bonded network structure. The applied basis set describes the H-bonds with good accuracy,[41] but the calculated

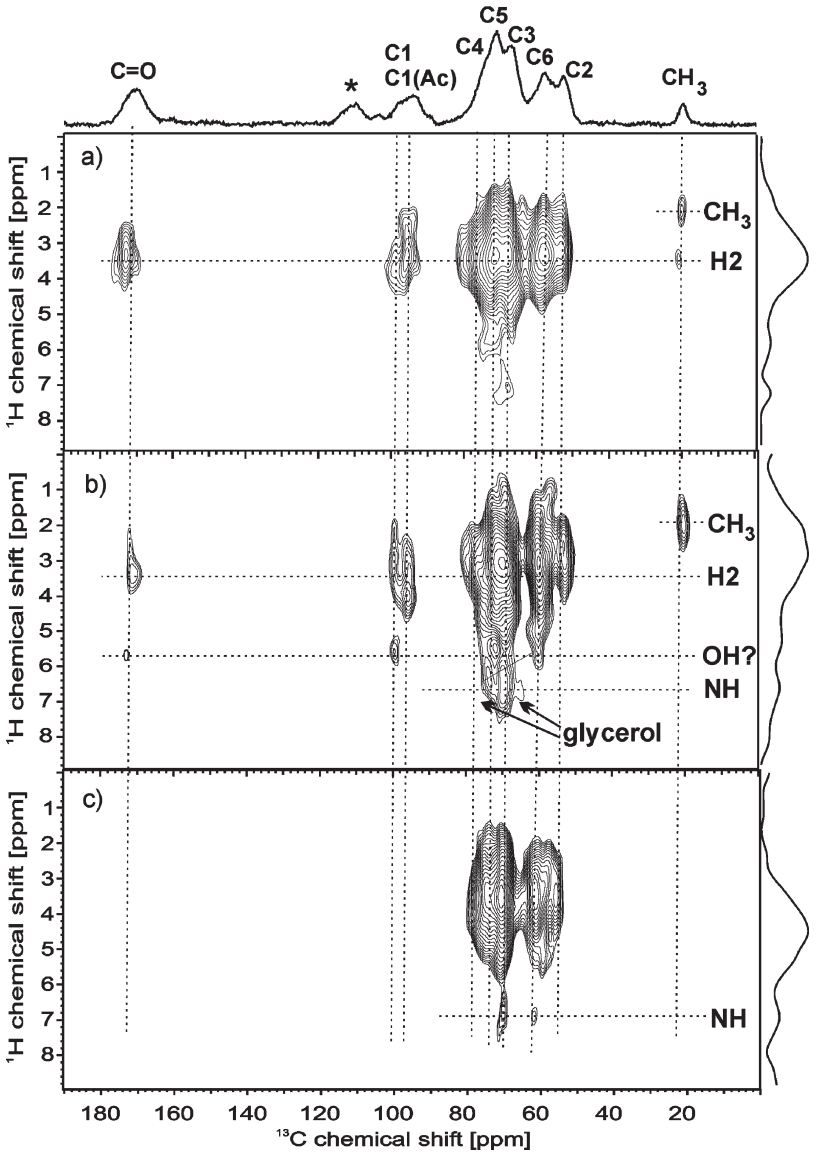

Figure 6. FSLG HETCOR spectra with a contact time of 500 μs (a, chitosan; b, chitosan + glycerol; c, chitosan + PEG 400). The contour levels are the same for all three spectra.

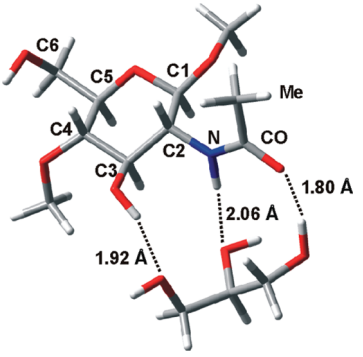

Figure 7. H-bonds between glycerol and chitosan.

energy values were not used because of the simplified model system. As Figure 7 shows, the glycerol molecule is able to form three H-bonds with the glucosamine unit. The creation of these H-bonds leads to immobilization of the glycerol and the acetamide groups so they cannot form intermolecular bonds between adjacent chitosan chains. The structure of the film is highly amorphous, and the structure shown in Figure 7 is only one possible form that may explain the cross-peaks in the HETCOR spectra. PEG 400 is able to form only one H-bond with chitosan, as our calculations with the same basis set showed (the PEG 400 was modeled with four EG units). The distance between the amide NH and the ether O atom was 2.15 Å, which suggests that the second-order bonds between the PEG 400 and chitosan molecules are much weaker than those between the glycerol and chitosan molecules.

Conclusions

Both glycerol and PEG 400 are good candidates as plasticizers of rigid and brittle chitosan films. Mechanical tests demonstrate that the plasticizing efficiencies of glycerol and PEG 400 are similar, although the breaking force for the film containing PEG 400 is larger than that for the glycerol-containing film. The three-dimensional H-bonded structure of chitosan changes when plasticizer materials are added to it, and the changes were investigated by means of solid-state NMR methods. Analysis of the Lee−Goldburg cross-polarization build-up curves revealed that glycerol decreases the mobility of the acetamide groups, which play a major role in the formation of H-bonds between adjacent chains. On the other hand, PEG 400 increases the

mobility of the acetamide groups. These plasticizer molecules therefore behave differently: while the glycerol molecules are immobilized in the chitosan matrix, PEG 400 remains mobile in the chitosan film. The two-dimensional $^{1}H-^{13}C$ FSLG HETCOR experiment supported the difference in mobility of the chitosan chains. Further, a specific interaction was observed between glycerol and the acetylglucosamine unit. This finding is an excellent illustration of the utility of the FSLG HETCOR experiment. Density functional theory calculations led to the finding that glycerol is able to form three H-bonds with a glucosamine unit, which supports the results of solid-state NMR experiments. We conclude that PEG 400 acts much more as an external plasticizer for chitosan films, while glycerol rather acts as an internal plasticizer.

Acknowledgment. We gratefully acknowledge the financial support from the Hungarian project GVOP-3.2.1.-2004-04-0210/3.0 for the NMR equipment. The preparation of the samples was supported by Hungarian Scientific Research Fund (OTKA) grant T-49815.

References and Notes

(1) Rinaudo, M. *Prog. Polym. Sci.* **2006**, *31*, 603–632.
(2) Kumar, M. N. V. R.; Muzzarelli, R. A. A.; Muzzarelli, C.; Sashiwa, H.; Domb, A. J. *Chem. Rev.* **2004**, *104*, 6017–6084.
(3) Okuyama, K.; Noguchi, K.; Miyazawa, T.; Yui, T.; Ogawa, K. *Macromolecules* **1997**, *30*, 5849–5855.
(4) Heux, L.; Brugnerotto, J.; Desbrieres, J.; Versali, M.-F.; Rinaudo, M. *Biomacromolecules* **2000**, *1*, 746–751.
(5) Ogawa, K.; Yui, T.; Okuyama, K. *Int. J. Biol. Macromol.* **2004**, *34*, 1–8.
(6) Webster, A.; Osifo, P. O.; Neomagus, H. W. J. P.; Grant, D. M. *Solid State Nucl. Magn. Reson.* **2006**, *30*, 150–161.
(7) Van de Velde, K.; Kiekens, P. *Carbohydr. Polym.* **2004**, *58*, 409–416.
(8) Kameda, T.; Miyazawa, M.; Ono, H.; Yoshida, M. *Macromol. Biosci.* **2005**, *5*, 103–106.
(9) Kono, H. *Biopolymers* **2004**, *75*, 255–263.
(10) Dodane, V.; Vilivalam, V. D. *Pharm. Sci. Technol. Today* **1998**, *1*, 246–253.
(11) Ofori-Kwakye, K.; Fell, J. T. *Int. J. Pharm.* **2003**, *250*, 431–440.
(12) Weerakody, R.; Fagan, P.; Kosaraju, S. L. *Int. J. Pharm.* **2008**, *357*, 213–218.
(13) Sinha, V. R.; Singla, A. K.; Wadhawan, S.; Kaushik, R.; Kumria, R.; Bansal, K.; Dhawan, S. *Int. J. Pharm.* **2004**, *274*, 1–33.
(14) Krauland, A. H.; Alonso, M. J. *Int. J. Pharm.* **2007**, *340*, 134–142.
(15) Fang, J. Y.; Chen, J. P.; Leu, Y. L.; Hu, H. W. *Eur. J. Pharm. Biopharm.* **2008**, *68*, 626–636.
(16) Hejazi, R.; Amiji, M. *J. Controlled Release* **2003**, *89*, 151–165.
(17) Wittaya-areekul, S.; Prahsarn, C. *Int. J. Pharm.* **2006**, *313*, 123–128.
(18) Aksungur, P.; Sungur, A.; Unal, S.; Iskit, A. B.; Squier, C. A.; Senel, S. *J. Controlled Release* **2004**, *98*, 269–279.
(19) Cervera, M. F.; Karjalainen, M.; Airaksinen, S.; Rantanen, J.; Krogars, K.; Heinemaki, J.; Colarte, A. I.; Yliruusi, J. *Eur. J. Pharm. Biopharm.* **2004**, *58*, 69–76.
(20) Lamim, R.; de Freitas, R. A.; Rudek, E. I.; Wilhelm, H. M.; Cavalcanti, O. A.; Bresolin, T. M. B. *Polym. Int.* **2006**, *55*, 970–977.
(21) Quijada-Garrido, I.; Iglesias-González, V.; Mazón-Arechederra, J. M.; Barrales-Rienda, J. M. *Carbohydr. Polym.* **2007**, *68*, 173–186.
(22) Suyatma, N. E.; Tighzert, L.; Copinet, A. *J. Agric. Food Chem.* **2005**, *53*, 3950–3957.
(23) Bajdik, J.; Marciello, M.; Caramella, C.; Domján, A.; Suvegh, K.; Marek, T.; Pintye-Hódi, K. *J. Pharm. Biomed. Anal.* **2009**, *49*, 655–659.
(24) Gaechter, R., Muller, H., Klemchuk, P. P., Eds. *Plastics Additives Handbook*, 4th ed.; Hanser/Gardner Publications: Cincinnati, 1993.
(25) Schmidt-Rohr, K.; Spiess, H. W. *Multidimensional Solid-State NMR and Polymers*, 3rd ed.; Academic Press: San Diego, CA, 1999.
(26) Brus, J.; Spirková, M.; Hlavatá, D.; Strachota, A. *Macromolecules* **2004**, *37*, 1346–1357.
(27) Anzai, K.; Kono, H.; Mizoguchi, J.; Yanagi, T.; Hirayama, F.; Arima, H.; Uekama, K. *Carbohydr. Res.* **2006**, *341*, 499–506.
(28) Hou, S. S.; Bonagamba, T. J.; Beyer, F. L.; Madison, P. H.; Schmidt-Rohr, K. *Macromolecules* **2003**, *36*, 2769–2776.
(29) Potrzebowski, M. J.; Helinski, J.; Olejniczak, S.; Ciesielski, W. *J. Phys. Org. Chem.* **2006**, *19*, 53–60.
(30) Mollica, G.; Geppi, M.; Pignatello, R.; Veracini, C. A. *Pharm. Res.* **2006**, *23*, 2129–2140.
(31) Geppi, M.; Guccione, S.; Mollica, G.; Pignatello, R.; Veracini, A. C. *Pharm. Res.* **2005**, *22*, 1544–1555.
(32) Maruta, K.; Kono, H.; Katoh, E.; Kuroki, S.; Ando, I. *Polymer* **2003**, *44*, 4021–4027.
(33) Bajdik, J.; Fehér, M.; Pintye-Hódi, K. *Appl. Surf. Sci.* **2007**, *253*, 7303–7308.
(34) Rossum, B. J. v.; Forster, H.; Groot, H. J. M. d. *J. Magn. Reson.* **1997**, *124*, 516–519.
(35) Lee, M.; Goldburg, W. I. *Phys. Rev. A* **1965**, *140*, 1261–1271.
(36) Massiot, D.; Fayon, F.; Capron, M.; King, I.; Le Calvé, S.; Alonso, B.; Durand, J. O.; Bujoli, B.; Gan, Z. H.; Hoatson, G. *Magn. Reson. Chem.* **2002**, *40*, 70–76.
(37) Fung, B. M.; Khitrin, A. K.; Ermolaev, K. *J. Magn. Reson.* **2000**, *142*, 97–101.
(38) van Rossum, B. J.; de Groot, C. P.; Ladizhansky, V.; de Groot, H. J. M. *J. Am. Chem. Soc.* **2000**, *122*, 3465–3472.
(39) Ladizhansky, V.; Vega, S. *J. Chem. Phys.* **2000**, *112*, 7158–7168.
(40) Frisch, M. J.; Trucks, G. W.; Schlegel, H. B.; Scuseria, G. E.; Robb, M. A.; Cheeseman, J. R.; Montgomery, J. A., Jr.; Vreven, T.; Kudin, K. N.; Burant, J. C.; Millam, J. M.; Iyengar, S. S.; Tomasi, J.; Barone, V.; Mennucci, B.; Cossi, M.; Scalmani, G.; Rega, N.; Petersson, G. A.; Nakatsuji, H.; Hada, M.; Ehara, M.; Toyota, K.; Fukuda, R.; Hasegawa, J.; Ishida, M.; Nakajima, T.; Honda, Y.; Kitao, O.; Nakai, H.; Klene, M.; Li, X.; Knox, J. E.; Hratchian, H. P.; Cross, J. B.; Adamo, C.; Jaramillo, J.; Gomperts, R.; Stratmann, R. E.; Yazyev, O.; Austin, A. J.; Cammi, R.; Pomelli, C.; Ochterski, J. W.; Ayala, P. Y.; Morokuma, K.; Voth, G. A.; Salvador, P.; Dannenberg, J. J.; Zakrzewski, V. G.; Dapprich, S.; Daniels, A. D.; Strain, M. C.; Farkas, O.; Malick, D. K.; Rabuck, A. D.; Raghavachari, K.; Foresman, J. B.; Ortiz, J. V.; Cui, Q.; Baboul, A. G.; Clifford, S.; Cioslowski, J.; Stefanov, B. B.; Liu, G.; Liashenko, A.; Piskorz, P.; Komaromi, I.; Martin, R. L.; Fox, D. J.; Keith, T.; Al-Laham, M. A.; Peng, C. Y.; Nanayakkara, A.; Challacombe, M.; Gill, P. M. W.; Johnson, B.; Chen, W.; Wong, M. W.; Gonzalez, C.; Pople, J. A. Gaussian 03, Revision C.02 ed.; Gaussian, Inc., Wallingford, CT, **2004**.
(41) Riley, K. E.; Op't Holt, B. T.; Merz, K. M. *J. Chem. Theory Comput.* **2007**, *3*, 407–433.